The B-spline Interpolation in Visualization

Željka Mihajlović[1] and Alan Goluban[2]

[1] Department of Electronics, Microelectronics, Computer and Intelligent Systems,
[2] Department of Control and Computer Engineering in Automation,
Faculty of Electrical Engineering and Computing, University of Zagreb, Zagreb, Croatia

The volume data is generally in the form of the large array of numbers. In order to render the object hidden in the volumetric data, we need to reconstruct or interpolate data values between the samples. The novelty presented in this paper is B-spline interpolation in the volumetric space. We show that this approach is better than currently used methods. We also present a hybrid approach, analyze this approach in frequency domain and compare it to B-spline interpolation.

To enhance the quality during the volume visualization process it is important to enhance the quality of the reconstruction. It is of crucial importance to explore different undesired effects. If better reconstruction is performed the more accurate result of volume visualization process is achieved.

Keywords: B-spline, volume rendering, volume reconstruction

1. Introduction

The volume visualization is based on the three-dimensional scalar or vector field. Object that should be visualized is represented by the array of discrete samples. During rendering of the object it is necessary to reconstruct the continuous three-dimensional function, defined by the samples, for any method applied. Classification of the methods for the volume visualization can be done regarding the space where they basically work. Development of the new methods extend the basic classification proposed by Kaufman [5]. There are three groups of methods: the object space methods, the image space methods and methods that are based on transformed object space.

The object space methods mainly create polygons or classic geometric primitives and project them in the projection plane [8]. Methods that are based on the image space start from the image plane and cast the rays from each picture element into the scene [7]. Methods that are based on the transformed object space work in transformed space, for example in the frequency domain [13] or in the wavelet domain [3]. There are also some hybrid methods that employ coherency characteristics from different spaces. The object space is first traversed to reorganize data to be prepared for traversing in the image space. During traversing the image space, rays are cast from each picture element in the object space [6]. Organization of the volume elements is very important, because significant performance benefits can be achieved if volume elements can be easily fetched along cast ray.

During the volume rendering there are several layers where reconstruction is necessary, and the error caused by reconstruction may occur. Reconstruction is done in the three-dimensional space based on the values of the volume elements. We must be able to interpolate the function at arbitrary locations to obtain the volume densities. Numeric integration along the ray path uses reconstructed values at sample points. To calculate the value assigned to the ray, values in the sample points along the ray are accumulated. Final reconstruction is done based on each ray in order to produce the final image (Fig. 1).

It is important to be aware of limitations of the reconstruction, because it can significantly influence the accuracy of the result. Investigation

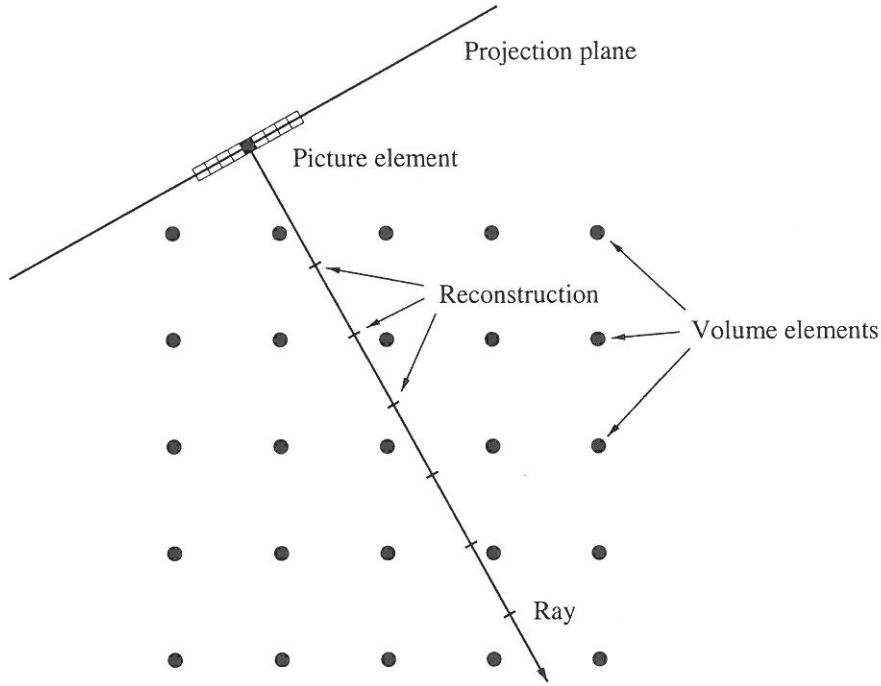

Fig. 1. Reconstruction in the volume rendering.

of the reconstruction or the interpolation is required to achieve compromise between different undesired artifacts and to accomplish optimal result.

2. Reconstruction in the Computer Graphics

Development of new rendering algorithms for visualization of the three-dimensional scalar fields is a recent area of research. Usually, related papers put the main accent on the proposal of new methods, while less attention is paid to the problem of reconstruction.

Aliasing is problem present in many areas of computer graphics. Objects are usually defined procedurally and they are synthetic. Prefiltering of such representation is not practical. Furthermore, transformation between continuous and discrete representation is often required. Aliasing may occur on every transformation of representations, and this problem also appears when resampling is required. Multilayer resampling is often required and each layer may cause additional error. This problem is well recognized in the computer graphics, and investigated by many authors.

Display of the computer-generated image is input object to our visual system, and it is not completely understood how our visual system works. Sensitivity of the human eye is specific, so minimal deviation in mathematical sense differs from the most pleasant result for our perceptual system. Even a little distortion in gray levels can cause unpleasant psychovisual result, especially in the areas with smooth changes.

In the analysis based on the perceptual approach, rather than mathematics, some authors prefer little aliasing in order to avoid other visual defects that result from trying to remove alias completely. The appearance of aliasing is investigated when family of piece-wise cubic filters is applied to image reconstruction [10]. Mitchell also presents [11] how stratified sampling reduces variance of the mean value of the image picture elements.

The problem is to numerically express the result that depends on our visual system. Marschner and Lobb [9] propose metric that can be used to measure the filter characteristics, in terms of smoothing and postaliasing. On the three-dimensional test signal they show the results, when different reconstructions are used. The proposed test function is highly sensitive to the aliasing, and different undesired effects are visible on the results. A disadvantage is in that the proposed test function is continuous, so drawback caused by discontinuity usual in real data

will not appear. In volume rendering, gradient information is used for shading and classification of the data set in combination with the voxel intensities. Bentum presents the analysis of gradient estimators in frequency domain, and proposes taking the derivative of the interpolation function itself [1].

Machiraju and Yagel characterize and measure error by applying Taylor series expansion. They characterize errors as truncation error and non-sinc error. The methods for error measurements are based on the spatial domain analyses. The Taylor series expansion of the convolution sum [12] leads to the quantitative and qualitative compression of the reconstruction and derivative filters. The analysis is based on the BC-splines defined by Mitchell.

It is important to distinguish approximation and interpolation approaches. The approximation curves are used to approximate control polygon, and interpolation curves must pass through the defined vertices. Toraichi used interpolation quadratic B-spline for image reconstruction [14], and Unser presented B-spline transforms for the image interpolation [15].

3. Prealiasing and Postaliasing

Volumetric space consists of volume elements. Each volume element may represent result from real world object sample, from numeric simulations, or may represent some pure mathematical value. The samples are taken from continuous space, but object with sharp edges in that space creates discontinuity. According to Shannon theory, signal can be reconstructed from its samples if two conditions are valid. First, spectrum of the signal must be bandlimited, and sampling frequency must be twice as high as the largest frequency present in the signal. The alias that occurs during sampling stage is called prealiasing and postaliasing is caused by the reconstruction.

Natural forms often contain discontinuity, so their spectrum is not bandlimited. Before sampling, lowpass filtering must be applied. If ideal (box) lowpass filtering is performed, Gibss phenomena will appear on each discontinuity. So, discontinuity creates unbandlimited spectrum. Therefore, ideal lowpass filter, used to eliminate higher frequencies, cause ringing effect near discontinuity. When discontinuity exists on piecewise linear function, Fourier series of function overshoots the function value near that discontinuity. Limes $\lim_{n\to\infty} S_n(f, x_n)$ of the *n-th* partial sum $S_n(f, x_n)$ of the Fourier series on the first local maximum (minimum) x_n near discontinuity converges to higher (lower) value than the value of the function. Wilbraham-Gibbs constant quantifies the degree of overshoot. On each side of discontinuity the limiting crest of the highest wave converges to 8,949% of the discontinuity height. This is an inherited property that should be taken into further consideration.

In the two-dimensions, ringing exhibits on every discontinuity in gray levels of the image. In the three-dimensions, volume elements escape over the edge of the object and create visual artifacts that manifest as clouds around the object. Some volume elements dive into the object creating caves in the object surface. To avoid ringing, continuous impulse response of the lowpass filter is required. Instead of box lowpass filtering, filters having smooth impulse response should be used. For lowpass filtering in two or three dimensions Gaussian filter will be used, although further detailed investigation is required.

Data acquisition can be achieved by different scanners: CT (Computer Tomography) or MR (Magnetic Resonance), for example. During the sampling process some lowpass filtering is performed, but information about it for the sequences of slices available on Internet, is usually unknown. If the sampling is not done correctly, information can be irrecoverably lost.

The resolution of scanned slices is usually high, but the number of slices is often insufficient because of radiation risks for the patient. To enlarge the number of slices, interpolation between the slices is required. Compression of the volume data is also desired because the size of dataset is large. Thus the reconstruction of the compressed volume, interpolation between slices, or interpolation of the volume elements become important steps.

The reconstruction is a term that is usually used in signal processing, and interpolation is a term used in mathematics or computer graphics. In this paper those two terms will be used interchangeably. Both approaches: one from the

interpolation of curves and the other from signal reconstruction, will be confronted in order to analyze the problem.

4. The B-spline Interpolation

When designing the curves and surfaces for CAD applications, some characteristic demands on the behavior of the curves and surfaces are required [2], [4]. The B-spline was created to fulfill certain requirements that will reflect very well in solving of our problem.

4.1. The Approximation B-spline

The approximation B-spline curve with degree k of each polynomial segment is defined with

$$\mathbf{p}(u) = \sum_{i=0}^{n} \mathbf{r_i}\, N_{i,k}(u)\,, \qquad (1)$$

where $\mathbf{r_i}$ are points of the control polygon, and $N_{i,k}(u)$ are called B-spline weight functions, or B-splines. The control polygon has $n+1$ control points. The $N_{i,k}(u)$ are defined based on knot sequence:

$$U_{knot} = \{u_0, u_1, \ldots u_m\}\,, \qquad (2)$$

with recursion formula:

$$N_{i,0}(u) = \begin{cases} 1, & u_i \le u \le u_{i-1} \\ 0, & otherwise, \end{cases} \qquad (3)$$

$$N_{i,k}(u) = \frac{(u-u_i)\, N_{i,k-1}(u)}{u_{i+k}-u_i} + \frac{(u_{i+k+1}-u)\, N_{i+1,k-1}(u)}{u_{i+k+1}-u_{i+1}}. \qquad (4)$$

When the denominator is equal to zero, fraction is assumed to have value of zero. In our consideration we restrict on the uniform case, where parametric intervals between successive knot values are equal to one, and with no multiple knot values.

$$U_{knot} = \{1, 2, 3, \ldots, m\}\,. \qquad (5)$$

In that uniform case, periodic segment can also be determined by the equation:

$$\beta_k(x) = \frac{1}{k!}\sum_{i=0}^{k+1}(-1)^i \binom{k+1}{i} \times \times\left(x - i + \frac{k+1}{2}\right)^k H\left(x - i + \frac{k+1}{2}\right), \qquad (6)$$

where k is degree of each polynomial segment and $H(x)$ is Heaviside step function. For further analysis the equation (6) can be rewritten with recursive relation:

$$\beta_k(x) = (\beta_{k-1} * \beta_0)(x)\,, \qquad (7)$$

where operator $*$ denotes convolution. If $\beta_k(x)$ is used for weight function, the approximation B-spline curve is:

$$\mathbf{p}(x) = \sum_{i=-\infty}^{\infty} \mathbf{r_i}\, \beta_k(x-i)\,, \qquad (8)$$

where $\mathbf{r_i}$ is infinite sequence of control points. For the uniform case, when $k = 3$ (cubic case), formulation of the *i-th* B-spline segment is:

$$\mathbf{p_i}(u) = \begin{bmatrix} u^3 & u^2 & u & 1 \end{bmatrix} \frac{1}{6} \cdot \begin{bmatrix} -1 & 3 & -3 & 1 \\ 3 & -6 & 3 & 0 \\ -3 & 0 & 3 & 0 \\ 1 & 4 & 1 & 0 \end{bmatrix} \begin{bmatrix} \mathbf{r_{i-1}} \\ \mathbf{r_i} \\ \mathbf{r_{i+1}} \\ \mathbf{r_{i+2}} \end{bmatrix}, \qquad (9)$$

where $u \in [0,\ 1)$. For the uniform cubic case derived from (1) and (4), or from the equation (6), four points control each segment. The segment of curve $\mathbf{p_i}(u)$ will approximate the control polygon.

Boundary conditions can be handled by using closed curves or circular repetition of the control points, by zero padding, or by setting some end conditions. For the sake of simplicity circular repetition of the control points will be applied. The derived form (9) is identical to the cubic BC-spline derived by Mitchell [10], by setting $B = 1,\ C = 0$:

$$k(x) = \frac{1}{6}\begin{cases} 3|x|^3 - 6|x|^2 + 4 & |x| < 1 \\ -|x|^3 + 6|x|^2 - 12|x| + 8 & 1 \le |x| < 2 \\ 0 & otherwise \end{cases}. \qquad (10)$$

With few arithmetic manipulations and reparameterization we can prove that (9) and (10)

represent the same reconstruction form. It is obvious that for the reconstruction in two dimensions (e.g. images) approximation spline causes blur, because smaller or greater values only approximate gray levels of the image. In spite of that, many authors use BC-spline defined by Mitchell [6], [1], [12]. In the three dimensions fine details are lost, and surface is smooth. The interpolation, as opposite to approximation of the control points, will significantly improve the resulting image.

The properties of the B-spline curves or surfaces extend in the image or volume reconstruction very well. These properties are continuity, convex hull, local control, variation diminishing and representation of the multiple values.

The convex hull property ensures that each point in the curve lies in the convex hull of no more than $k+1$ nearby control points. Thus, sample points bound the space of the reconstructed curve, surface or volume, so reconstructed values will not escape outside the convex hull. The local control property makes far points less influential on the segment of consideration. In terms of signal processing the local control property implies narrow impulse response of the reconstruction filter. The impulse response of ideal reconstruction filter is sinc function, which is very wide. The points far from the point of reconstruction can have undesired influence.

Variation diminishing property prevents variations of the curve, or variations in the gray levels of the reconstructed image. The curve is not intersected by any straight line (or plane) more often than the control polygon. For a cubic case, control polygon consists of the four control points and there are at most three intersections between straight line and curve. This property is very important in the image reconstruction, because the human eye is very sensitive to small changes of the intensity, especially in the areas where gray levels are changing smoothly.

4.2. The B-spline Interpolation

To build the B-spline interpolation it is crucial to find the control polygon of the B-spline approximation, such that the resultant curve passes through the requested points. For the cubic uniform closed curve, the matrix form defines points of the control polygon:

$$\begin{bmatrix} \mathbf{p}_0 \\ \mathbf{p}_1 \\ \cdots \\ \mathbf{p}_{n-2} \\ \mathbf{p}_{n-1} \end{bmatrix} = \frac{1}{6} \begin{bmatrix} 4 & 1 & 0 & \ldots & 0 & 0 & 1 \\ 1 & 4 & 1 & \ldots & 0 & 0 & 0 \\ & \cdots & & \cdots & & \cdots & \\ 0 & 0 & 0 & \ldots & 1 & 4 & 1 \\ 1 & 0 & 0 & \ldots & 0 & 1 & 4 \end{bmatrix} \begin{bmatrix} \mathbf{r}_0 \\ \mathbf{r}_1 \\ \cdots \\ \mathbf{r}_{n-2} \\ \mathbf{r}_{n-1} \end{bmatrix}, \tag{11}$$

where $\mathbf{p_i}$ is the known sequence of points that must be interpolated, and $\mathbf{r_i}$ is an unknown sequence of points of the control polygon. This expression also describes a circular convolution. Evaluation of the inverse threediagonal matrix or the LU-decomposition can be applied to find $\mathbf{r_i}$. The resulting points $\mathbf{r_i}$ are used in equation (1) to find the interpolating function. To facilitate the analysis it is convenient to consider the convolution form (8) in the frequency domain. From this equation in the frequency domain we can show that:

$$P(\omega) = R(\omega)B_k(\omega), \tag{12}$$

where $P(\omega)$, $R(\omega)$ *and* $B_k(\omega)$ are Fourier transforms of $\mathbf{p}(x)$, $\mathbf{r}$ *and* $\beta(x)$ respectively. This suggests that spline coefficients can be determined by the inverse filtering:

$$R(\omega) = S_k(\omega)P(\omega) = \frac{1}{B_k(\omega)}P(\omega). \tag{13}$$

Using equation (13) we can also determine frequency response of the B-spline interpolation (17).

4.3. Hybrid Reconstruction

In the volume visualization reconstruction is usually done with trilinear interpolation in the sample point. Trilinear interpolation is simple and it is not time consuming, because it uses only eight neighboring elements for the computation of the reconstructed value. In further analysis we reconstruct a function from sample points in two ways. The first approach is hybrid, and the idea is to magnify the volume element space two times in each coordinate direction, using B-spline interpolation. After magnification, trilinear interpolation is used during the volume rendering. The second approach is based on direct implementation of the B-spline interpolation in the volume visualization algorithm. In the second approach 64 neighboring

elements are required for the computation of each reconstructed value, but the volume element space is eight times smaller than in the previous case. Frequency responses of these two approaches will be derived to emphasize the difference, which us usually neglected.

In order to compare these two approaches we derive the frequency response for one-dimensional case. Frequency response of the $\beta_0(x)$ is:

$$B_0(\omega) = \frac{\sin\left(\frac{\omega}{2}\right)}{\frac{\omega}{2}} = \operatorname{sinc}\left(\frac{\omega}{2\pi}\right). \qquad (14)$$

Frequency response of the B-spline approximation can easily be determined from (7):

$$B_k(\omega) = \operatorname{sinc}^{k+1}\left(\frac{\omega}{2\pi}\right). \qquad (15)$$

In order to find frequency response for the B-spline interpolation we have to determine $S_k(\omega)$ in (13). For the B-spline interpolation, prefiltering is required in order to find appropriate control polygon for the B-spline approximation. Frequency response of the prefiltering is:

$$S_k(\omega) = \frac{1}{B_k(\omega)} = \frac{1}{\beta_k(0) + 2\sum_{i=1}^{\lfloor \frac{k}{2} \rfloor} \beta_k(i)\cos(i\omega)}. \qquad (16)$$

Frequency response of B-spline interpolation is defined by frequency response of prefiltering $S_k(\omega)$ and with frequency response of B-spline approximation (15). For the cubic case, when $k = 3$ frequency response of the B-spline interpolation is:

$$S_3(\omega)B_3(\omega) = \frac{3\operatorname{sinc}^4\left(\frac{\omega}{2\pi}\right)}{2 + \cos(\omega)}. \qquad (17)$$

For the hybrid approach the volumetric space is first enlarged eight times (two times in each

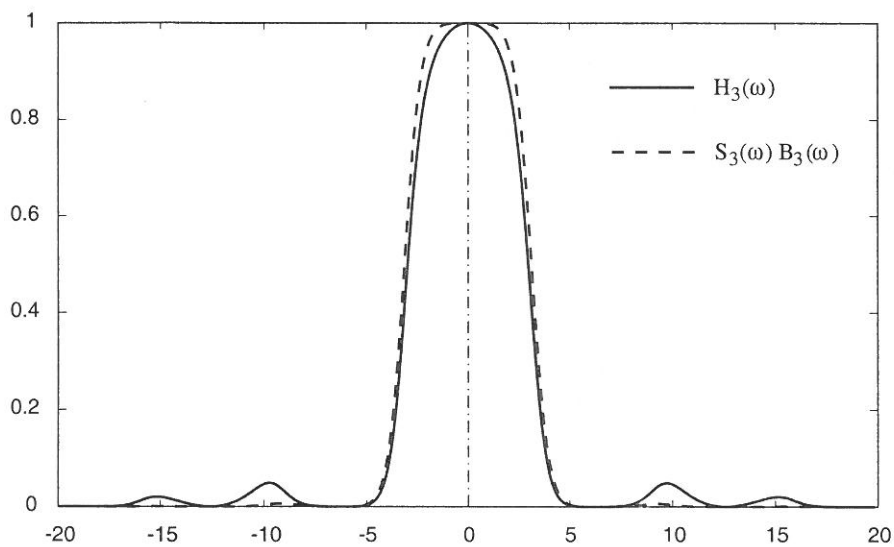

Fig. 2. Frequency responses of hybrid reconstruction (18) and direct implementation of B-spline interpolation (17).

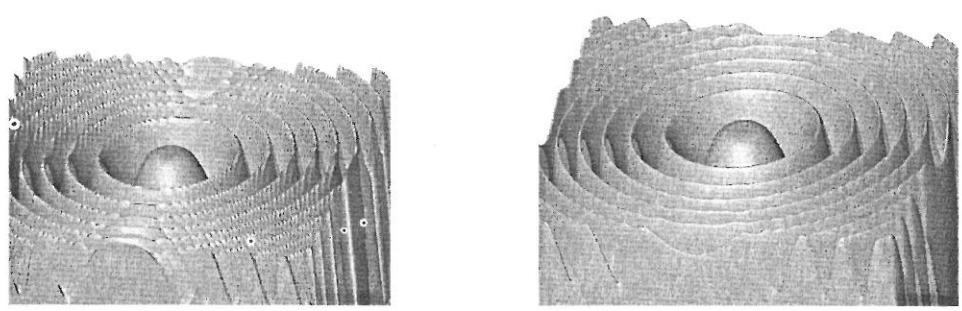

Fig. 3. Three-dimensional example of a) hybrid approach and b) direct implementation of B-spline interpolation.

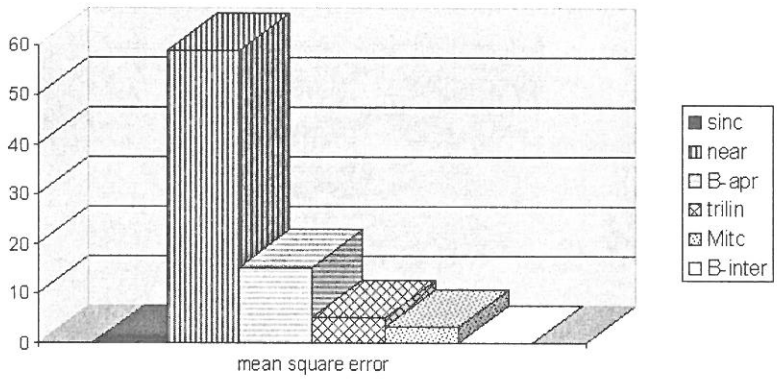

Fig. 4. Six different reconstructions: reconstruction with sinc, nearest neighbor, 3-rd order B-spline approximation, linear interpolation, Mitchell reconstruction with $B = C = 1/3$ and 3-rd order B-spline interpolation.

direction) and then rendering with trilinear interpolation is applied. Frequency response of this hybrid reconstruction is:

$$H_3(\omega)=\text{sinc}^2\left(\frac{\omega}{4\pi}\right)\cos^4\left(\frac{\omega}{4}\right)\frac{2+\cos\left(\frac{\omega}{2}\right)}{2+\cos(\omega)}. \tag{18}$$

Figure 2 illustrates frequency responses of these two approaches. It is obvious that direct B-spline has better passband and stopband characteristics. Although the direct implementation of B-spline interpolation is better, overall characteristics of the hybrid reconstruction, when compared to other reconstruction methods, imply that the hybrid reconstruction is also acceptable.

Figure 3.a illustrates a three-dimensional object reconstructed by the hybrid method, while figure 3.b shows the result of direct implementation of the B-spline interpolation.

5. Results

Six different reconstruction filters in the two and three-dimensional space are used. Applied reconstructions are: sinc function, nearest

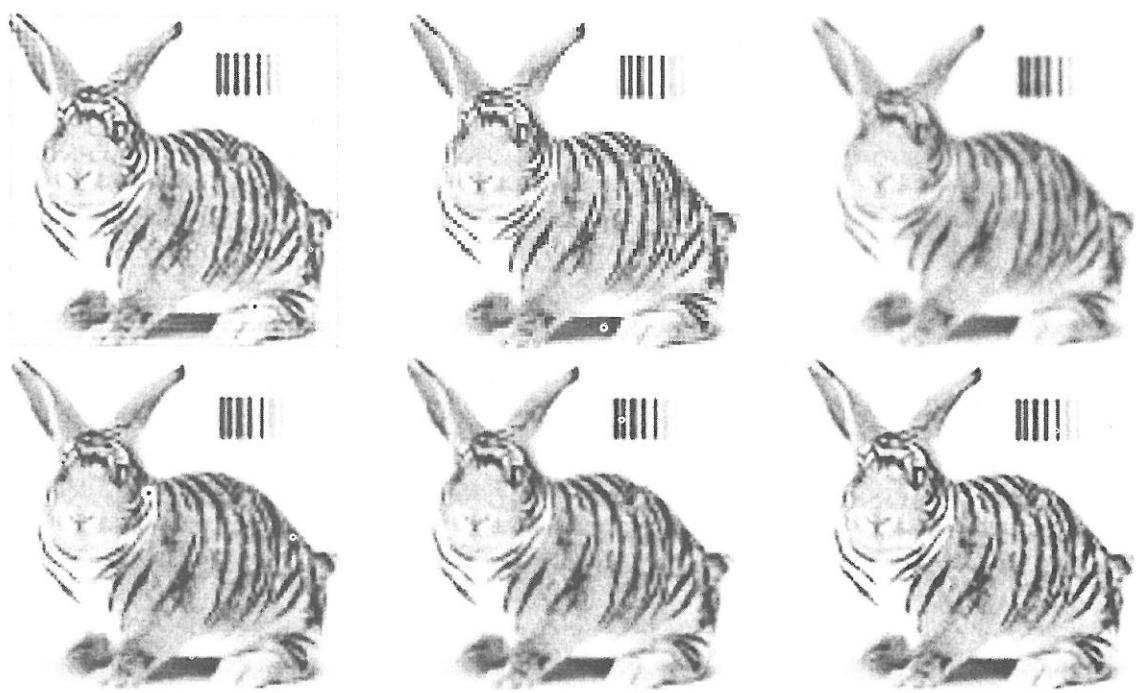

Fig. 5. Six different reconstruction methods in 2D. a) reconstruction with sinc function, b) nearest neighbor, c) 3-rd order B-spline approximation, d) linear interpolation, e) Mitchell reconstruction with $B = C = 1/3$ and f) 3-rd order B-spline interpolation.

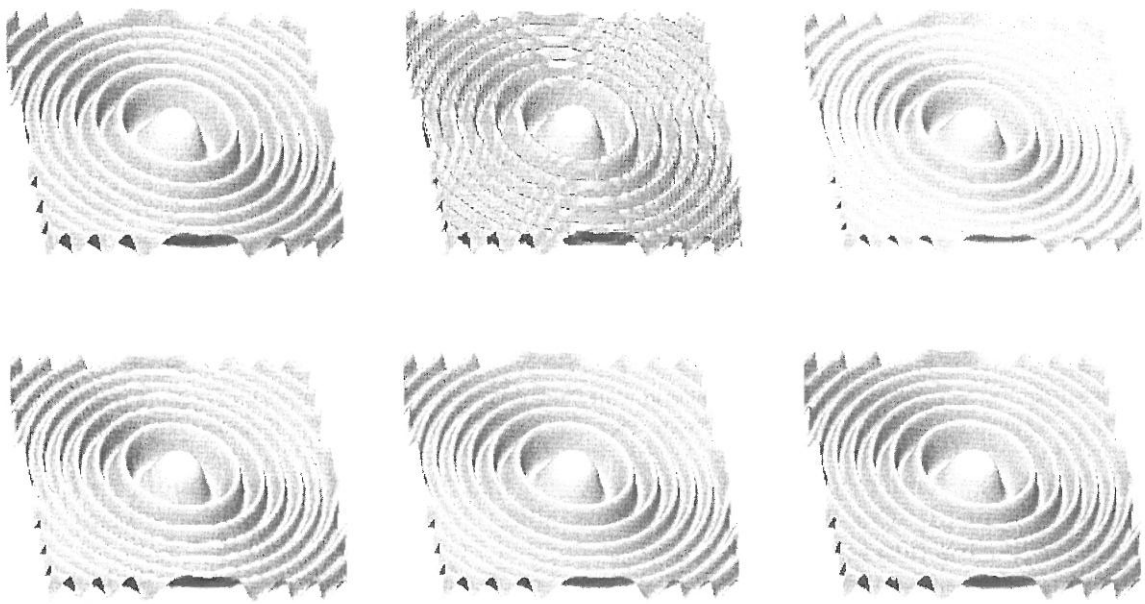

Fig. 6. Six different reconstruction methods in 3D. a) reconstruction with sinc function, b) nearest neighbor, c) 3-rd order B-spline approximation, d) linear interpolation, e) Mitchell reconstruction with $B = C = 1/3$ and f) 3-rd order B-spline interpolation.

neighbor, B-spline approximation, three-linear interpolation, Mitchell reconstruction with BC-spline $B = C = 1/3$ and B-spline interpolation. Reconstruction error is measured between initial and reconstructed objects as mean square error (Fig. 4).

Reconstruction with sinc function exhibits strong ringing artifact, although mean square error is minimal. Nearest neighbor interpolation (Fig. 5.b 6.b) exhibits strong artifacts. Third order B-spline approximation is very blurred (Fig. 5.c). In three dimensions the reconstructed waves get shallower (Fig. 6.c). Trilinear interpolation causes variations in the height of the circular crests (Fig. 6.d). Reconstruction kernel proposed by Mitchell is of the same size as the B-spline interpolation. In the 2D images reconstructed with B-spline interpolation the result is sharper than the image reconstructed using Mitchell kernel. In the three-dimensional space the difference is in sharper and darker shadows on the waves. The best result is achieved for the B-spline interpolation.

Further illustrations are made for the hybrid approach. In visualization programs trilinear interpolation is usually used, and optimization is often done for this interpolation. If we want to enhance quality of the result, volume can be enlarged and then rendered with trilinear interpolation. Direct implementation of the B-spline interpolation yields better result, but it can be also used to enlarge volume and enhance the quality when visualization programs with trilinear interpolation are used.

The two-dimensional examples (Fig. 5) and the three-dimensional examples (Fig. 6) of the six reconstruction methods are presented. For the three-dimensional example the test function proposed by Marshner and Lobb [9] is used.

Acknowledgment

This work has been carried out within the project 036014 Problem-Solving Environments in Engineering, funded by Ministry of Science and Technology of the Republic of Croatia.

References

[1] M. J. BENTUM, B. A. LICHTENBELT, T. MALZBENDER, Frequency Analysis of Gradient Estimators in Volume Rendering, *IEEE Transactions on Visualization*, Vol. 2, No. 3, (1996), pp. 242–253.

[2] G. FARIN, *Curves and Surfaces for Computer Aided Geometric Design, a Practical Guide,* Academic Press, Harcourt Brace Jovanovich Publishers, Boston, 1990.

[3] M. H. GROSS, L. LIPPERT, R. DITTRICH, S. HARING, Two Methods for Wavelet-Based Volume Rendering, Technical Report, No. 247, Computer Science Department, (1996), ETH Zurich.

[4] N. GUID, B. ŽALIK, Contribution to practical Consideration of B-splines, *Automatika,* Vol. 31, No. 1–2, (1990), pp. 83–88.

[5] A. KAUFMAN, 3D Volume Visualization, *Eurographics '90,* Tutorial Note 12, 1990.

[6] P. LACROUTE, Fast Volume Rendering Using Shear-Warp Factorization of the Viewing Transformation, (1995), Technical Report: CSL–TR–95–678.

[7] M. LEVOY, Display of Surfaces from Volume Data, *Proc. IEEE Computer Graphics and Applications,* Vol. 8, No. 3, (1988), pp. 29–37.

[8] W. E. LORENSEN, H. E. CLINE, Marching Cubes: A High Resolution 3D Surface Construction Algorithm, *Computer Graphics,* Vol. 21, No. 4, (1987), pp. 163–169.

[9] S. R. MARSHNER, R. J. LOBB, An Evaluation of Reconstruction Filters for Volume Rendering, *Proc. Visualization '94,* (1994), pp. 100–107.

[10] D. P. MITCHELL, A. N, NETRAVALI, Reconstruction Filters in Computer Graphics, *Computer Graphics,* Vol. 22, Number 4, (1988), pp. 221–228.

[11] D. P. MITCHELL, Consequences of Stratified Sampling in Graphics, *Computer Graphics,* SIGGRAPH '96 Proceeding, (1996), pp. 277–280.

[12] T. MOLLER, R. MACHIRAJU, K. MULLER, R. YAGEL, Evaluation and Design of Filters Using Taylor Series Expansion, *IEEE Transactions on Visualization and Computer Graphics,* Vol. 3, No. 2, (1997), pp. 184–199.

[13] T. TOTSUKA, M. LEVOY, Frequency Domain Volume Rendering, *Computer Graphics,* SIGGRAPH '93 Proceeding, (1993), pp. 271–278.

[14] K. TORAICHI, S. YANG, M. KAMADA, R. MORI, Two-dimensional Spline Interpolation for Image Reconstruction, *Pattern Recognition,* Vol. 21, No. 3, (1988), pp. 275–284.

[15] M. UNSER, A. ALDROUBI, M. EDEN, Fast B-Spline Transforms for Continuous Image Representation and Interpolation, *IEEE Transactions on PAMI,* Vol. 13, No. 3, (1991), pp. 277–285.

Received: February, 1999
Accepted: April, 1999

Contact address:

Željka Mihajlovi
Department of Electronics, Microelectronics,
Computer and Intelligent Systems,
Faculty of Electrical Engineering and Computing
University of Zagreb
Unska 3
10 000 Zagreb
Croatia
e-mail: zeljka.mihajlovic@fer.hr

Alan Goluban
Department of Control and Computer Engineering in Automation
Faculty of Electrical Engineering and Computing
University of Zagreb
Unska 3
10 000 Zagreb
Croatia
e-mail: alan.goluban@fer.hr

ŽELJKA MIHAJLOVIĆ received her BS and MS degrees in electrical engineering from the Faculty of Electrical Engineering and Computing, University of Zagreb, in 1988 and 1993 respectively. In 1997 she obtained her Ph.D. in electrical engineering, also from the Faculty of Electrical Engineering and Computing. Her thesis was about interpolation and reconstruction in visualization of volume data. Currently she is working as a research and teaching assistant at the Department of Electronics, Microelectronics, Computer and Intelligent Systems, Faculty of Electrical Engineering and Computing, University of Zagreb. Her main research interests include computer graphics, particular visualization and signal processing applied to volume rendering.

ALAN GOLUBAN received his BS degree in electrical engineering from the Faculty of Electrical Engineering and Computing, University of Zagreb in 1995. In 1998 he received his MS in electrical engineering, also from Faculty of Electrical Engineering and Computing. He is currently working as research and teaching assistant at the Department of Control and Computer Engineering in Automation. His professional interests include volume rendering in frequency domain, and genetic algorithms.